THE ASTROPHYSICAL JOURNAL, 553:L137–L140, 2001 June 1
© 2001. The American Astronomical Society. All rights reserved. Printed in U.S.A.

A SHORT-TIMESCALE CANDIDATE MICROLENSING EVENT IN THE POINT-AGAPE PIXEL LENSING SURVEY OF M31

M. AURIÈRE,[1] P. BAILLON,[2] A. BOUQUET,[3] B. J. CARR,[4] M. CRÉZÉ,[3,5] N. W. EVANS,[6] Y. GIRAUD-HÉRAUD,[3] A. GOULD,[3,7] P. C. HEWETT,[8] J. KAPLAN,[3] E. KERINS,[6] E. LASTENNET,[4,9] Y. LE DU,[6] A.-L. MELCHIOR,[4,10] S. PAULIN-HENRIKSSON,[3] S. J. SMARTT,[8] AND D. VALLS-GABAUD[11]

Received 2001 February 5; accepted 2001 April 24; published 2001 May 16

ABSTRACT

We report the discovery of a short-duration microlensing candidate in the northern field of the POINT-AGAPE pixel lensing survey toward M31. Almost certainly, the source star has been identified on *Hubble Space Telescope* archival images, allowing us to infer an Einstein crossing time of $t_{\rm E} = 10.4$ days, a maximum magnification of $A_{\rm max} \sim 18$, and a lens-source proper motion $\mu_{\rm rel} > 0.3$ μas day^{-1}. The event has a projected separation of 8′ from the center of M31, beyond the bulk of the stellar lens population. There are three plausible identifications/locations for the lensing object: a massive compact halo object (MACHO) in either M31 or the Milky Way, or a star in the M31 disk. The most probable mass is 0.06 $M_\odot$ for an M31 MACHO, 0.02 $M_\odot$ for a Milky Way MACHO, and 0.2 $M_\odot$ for an M31 stellar lens. While the stellar interpretation is possible, the MACHO interpretation is the most probable for halo fractions above 20%.

Subject headings: galaxies: halos — galaxies: individual (M31) — gravitational lensing — stars: variables: other

1. INTRODUCTION

Following the suggestions of Crotts (1992) and Baillon et al. (1993), the POINT-AGAPE collaboration[12] has embarked on a pixel lensing survey of M31 using the Wide Field Camera (WFC) on the 2.5 m Isaac Newton Telescope (INT). The high inclination of M31's disk causes an asymmetry in the observed rate of microlensing by lenses in a spheroidal halo (Crotts 1992). We are monitoring two fields of 0.3 deg^2 each, located to the north and south of the center of M31. The survey has the potential to map the global distribution of microlensing events in M31 and to quantify any large-scale gradient. The main difficulties are that the M31 sources are resolved only while they are lensed (and then only if the magnification is substantial) and that seeing causes substantial variations in the point-spread function. The pixel lensing technique has been developed to cope with these problems (Crotts & Tomaney 1996; Ansari et al. 1997, 1999). POINT-AGAPE is a long-term program, as at least 3 yr of data will be required to make a convincing identification of any gradient (Kerins et al. 2001). Also, it is necessary to establish a long time baseline to distinguish microlensing events from variable stars. In this Letter, we report on a particularly interesting and convincing early candidate, PA-99-N1, so named because it is the first event to be announced by POINT-AGAPE that peaked in the northern field in 1999.

2. OBSERVATIONS AND DATA ANALYSIS

Observations were obtained in two bands, Sloan r' and g', spanning 1999 August to December. We restrict analysis to a (11′ × 22′) field centered 3′ west and 12′ north of the center of M31. Exposure times were typically 10 minutes per field per night. The observations are strongly clustered because the WFC was not always mounted on the telescope. Data reduction is described in detail elsewhere (Ansari et al. 1997; Le Du 2000). Following standard preprocessing procedures, each image is geometrically and photometrically aligned relative to a reference image (taken on 1999 August 14), chosen because it has a long exposure time, typical seeing (1.″6), and little contribution to the sky background from the Moon. The light curves are computed by summing the flux in 7 pixel (2.″3) square "superpixels" and then removing the correlation due to seeing variations. The superpixel size is set by the poorest seeing, ~2.″1.

Event detection is performed using the r'-band frames, which have better temporal sampling and smaller variations in sky background. We use simple selection criteria designed to isolate high signal-to-noise ratio (S/N) events. The pixel light curves are searched for the presence of bumps, defined by at least four consecutive data points rising above the background by a minimum of 4 σ. The significance of a detection is quantified by the probability P of obtaining data points, each of which has at least the S/N of the measured points. Candidate microlensing events are defined to possess only one bump with $-\ln P > 100$ and no other bump with $-\ln P > 20$ (see Ansari et al. 1997). The background employed is the minimum of averages computed over any seven consecutive data points. Microlensing parameters are estimated from a simultaneous fit of a high-magnification degenerate microlensing curve to the data in both the r' and g' bands (Gould 1996). A candidate event is retained providing that the reduced $\chi^2 < 3$ and a flux excess of at least 1 ADU s^{-1} is

[1] Laboratoire d'Astrophysique UMR 5572, Observatoire Midi-Pyrénées, 57 Avenue d'Azereix, BP 826, F-65008 Tarbes Cedex, France.
[2] CERN, Genève 23, CH-1211, Switzerland.
[3] Laboratoire de Physique Corpusculaire et Cosmologie, Collège de France, 11 Place Marcelin Berthelot, F-75231 Paris, France.
[4] Astronomy Unit, School of Mathematical Sciences, Queen Mary and Westfield College, Mile End Road, E1 4NS London, UK.
[5] Université de Bretagne-Sud, Campus de Tohannic, BP 573, F-56017 Vannes Cedex, France.
[6] Theoretical Physics, Department of Physics, 1 Keble Road, OX1 3NP Oxford, UK.
[7] Department of Astronomy, Ohio State University, 140 West 18th Avenue, Columbus, OH 43210.
[8] Institute of Astronomy, Madingley Road, CB3 0HA Cambridge, UK.
[9] Departamento de Astronomia, UFRJ, Ladeira do Pedro Antônio 43, 20080-090 Rio de Janeiro RJ, Brazil.
[10] DEMIRM UMR 8540, Observatoire de Paris, 61 Avenue Denfert-Rochereau, F-75014 Paris, France.
[11] Laboratoire d'Astrophysique, UMR CNRS 5572, Observatoire Midi-Pyrénées, 14 Avenue Edouard Belin, F-31400 Toulouse, France.
[12] See http://www.point-agape.org.

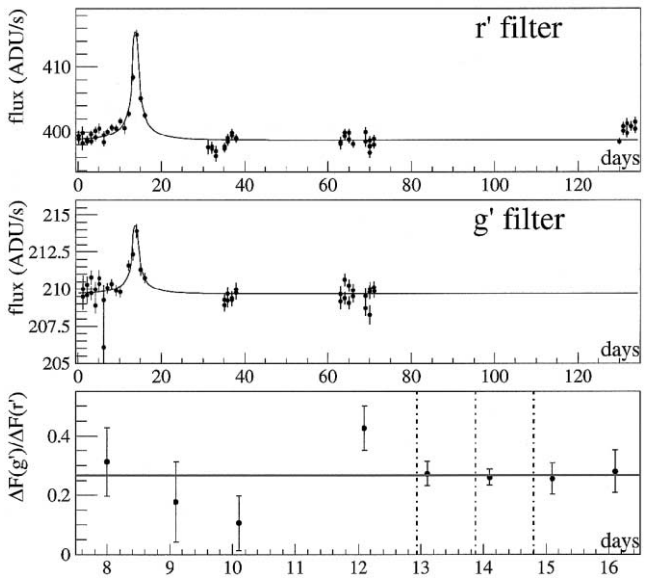

FIG. 1.—Panels (*a*) and (*b*) show the flux in r' and g' against time in units of days. Panel (*c*) is a zoom, including the event, that shows the variation of the ratio of the flux change in the two passbands $\Delta F_{g'}/\Delta F_{r'}$ with time. The vertical lines are centered on t_0 and are separated by 0.9 days, i.e., half the FWHM. Time is in units of days, equal to J − 2,451,392.5, where J is the Julian Date.

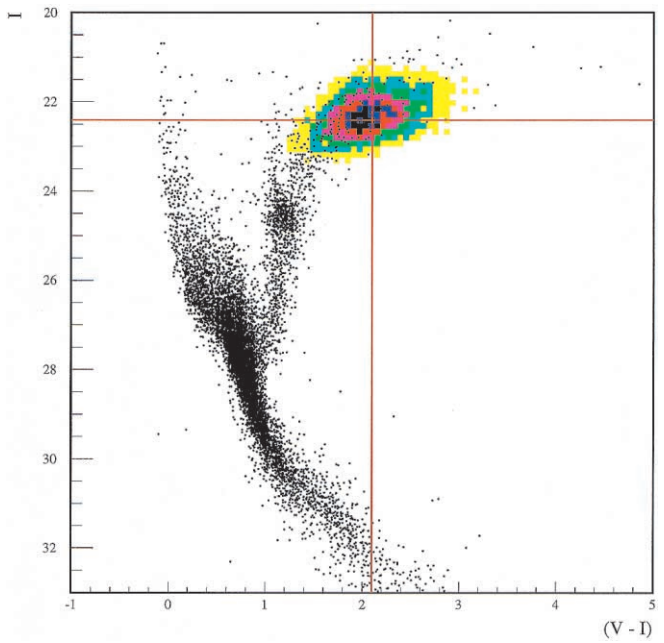

FIG. 2.—Superposition of the *Hipparcos* (*dots*) and *HST* (*shaded area*) color-magnitude diagrams. The *Hipparcos* stars have been moved to the position of M31 [assuming $(m-M)_0 = 24.43$ and total estimated extinction $A_V = 0.4$]. The intersection of the horizontal and vertical lines shows the position of the *HST* object.

observed in the g' band. To reduce the number of false positives due to other forms of stellar variability, we further require that the parameters of the microlensing fit satisfy $t_{1/2} < 8$ days with a peak r'-band flux greater than 10 ADU s^{-1}, corresponding to $R_{\rm peak} < 21.5$. One candidate, with $t_{1/2} \sim 1.8$ days, satisfies the criteria.

3. THE MICROLENSING CANDIDATE

Figure 1 shows the light curves in r' and g' of this candidate together with the nondegenerate fit derived below. The g' data with large error bars were taken on nights with a significant amount of moonlight. Using the Aladin Sky Atlas,[13] we find that PA-99-N1 has a J2000 position: $\alpha = 00^{\rm h}42^{\rm m}51\overset{\rm s}{.}42$, $\delta = +41°23'53\overset{''}{.}7$, placing it $7'52''$ from the center of M31, projected on the near disk. Using DAOPHOT (Stetson 1987) on the images taken nearest maximum magnification, we find $R = 20.80 \pm 0.13$ and $V = 22.00 \pm 0.17$, i.e., $V-R = 1.20 \pm 0.22$ and $M_V = -2.8 \pm 0.3$, assuming $(m-M)_{0,\,\rm M31} = 24.43$ and estimated total extinction $A_V = 0.4 \pm 0.2$. The transformation from instrumental (r', g') to Johnson (V, R) is based on 31 standard stars that lie in the same field as PA-99-N1 (Magnier et al. 1993; Haiman et al. 1994). Microlensing events are achromatic, so the ratio of flux *change* in different bands should be constant in time (e.g., Ansari et al. 1997). This requires

$$\frac{\Delta F_{g'}(t)}{\Delta F_{r'}(t)} = \frac{F_{g'}(t) - F_{{\rm base},\,g'}}{F_{r'}(t) - F_{{\rm base},\,r'}} = \text{constant}, \qquad (1)$$

which does indeed hold for PA-99-N1 (see Fig. 1*c*).

Hubble Space Telescope (*HST*) is capable of detecting giant branch stars in M31. Since the microlensing event is very red, $V-R \sim 1.2$, the source must lie either high up on the giant branch, where essentially all stars are resolved by *HST*, or on the main sequence and so magnified by $A_{\rm max} \gtrsim 10^4$ (see Fig. 2). The latter possibility is extremely unlikely a priori. Hence, a firm prediction of the microlensing interpretation is that a star with the same color should be visible in suitable *HST* images. The position of PA-99-N1 lies within a series of five (*HST*) Wide Field Planetary Camera 2 archival images taken in 1996 July, three with the F814W (∼*I*) filter and two with the F606W (∼*V*) filter. We use the relations of Zheng et al. (2001) to transform from these filters to Johnson-Cousins *V* and *I*. The spatial transformation between the INT and *HST* frames is derived by comparing the positions of the eight stars that are both resolved in the INT image and unsaturated in the *HST* image. The uncertainty in this transformation is small, and the error in the position of the candidate is dominated by the 0.2 pixel ($0\overset{''}{.}07$) uncertainty in measuring the location of the candidate itself on the INT frames. On the *HST* frames, within the 1 σ positional error circle centered on the event, there is a resolved star for which we find $V = 24.51 \pm 0.12$ and $I = 22.41 \pm 0.10$, implying $V-I = 2.10 \pm 0.16$. There are no other resolved stars visible within $0\overset{''}{.}21$ (3 σ). For typical stellar populations, this $V-I$ is compatible with the $V-R = 1.20 \pm 0.22$ measured for the event (Demarque et al. 1996). The prior probability to find such a star so close to the predicted position is only 3%. We conclude that the object in the *HST* frames is almost certainly the source star of the event.

4. LIGHT-CURVE INTERPRETATION

4.1. *PA-99-N1 as a Variable Star*

Can the light curve be due to a variable star? The color and magnitude are compatible with an M0 Mira at maximum. However, such Mira variables have periods greater than 200 days, and their flux at maximum does not vary as rapidly as the event (Cox 2000). PA-99-N1 is unlikely to be a dwarf nova. It is too bright at maximum to be in M31. If it is a Galactic dwarf nova,

[13] See http://aladin.u-strasbg.fr/aladin.gml.

TABLE 1
FIT PARAMETERS FOR PA-99-N1

N	χ^2	t_0 (days)	u_0	t_E (days)	$F_{s,r'}$ (ADU s^{-1})	$F_{s,g'}$ (ADU s^{-1})	$F_{b,r'}$ (ADU s^{-1})	$F_{b,g'}$ (ADU s^{-1})
97	154	13.87 ± 0.04	0.056 ± 0.009	10.4 ± 1.5	1.02 ± 0.17	0.28 ± 0.05	397.65 ± 0.18	209.40 ± 0.10

NOTE.—N: number of points; t_0: time of the peak; u_0: impact parameter; t_E: Einstein timescale; F_s and F_b: source and background fluxes in two bands. The maximum magnification is $A_{max} \sim u_0^{-1} \sim 18$.

it must be either unusually faint or improbably far from us (>10 kpc). It is also unlikely to be a nova. The brightness decrease of PA-99-N1 just after maximum is very rapid, with a rate of decline of about 0.7 mag day^{-1}. Capaccioli et al. (1989) studied the relation between the rate of decline and the magnitude at maximum for novae in M31 and found that the brighter the nova, the faster the decrease. The decline of PA-99-N1 would indicate a nova as bright as $V = 16$, which would imply $A_V = 6$, in stark contrast to the small extinction required by Figure 2. To conclude, there is no type of stellar variability known to us that could generate the light curve of PA-99-N1.

The candidate selection criteria (§ 2) ensured that only one significant "bump" was present in the observations taken during the 1999 observing season. Examination of additional frames, taken with the 1.3 m telescope at the MDM observatory, shows no evidence for variability during the 1998 and 1999 observing seasons. However, if the weak bump evident in 1999 December, near day 130 in Figure 1, were due to the event source, one would have to conclude that the source was probably a variable. Further investigation of the December images is encouraging; for each of the nine images in December, we identify a comparison image, from earlier in the season, with similar seeing and subtract the image pairs. Summing these difference images, we find a very clear stellar profile located 1.″1 ± 0.″1 south of the source. Hence, the feature appears to be due to stellar variability from a star close enough to contaminate our 2.″3 superpixels but clearly distinguishable from the event source.

4.2. *PA-99-N1 as a Microlensing Event*

Making use of the identification of the *HST* star as the source of the microlensing event, we fit the data to a full (nondegenerate) microlensing curve and so evaluate the Einstein crossing time, $t_E = 10.4$ days. By permitting the measurement of $t_E = \theta_E/\mu_{rel}$, where $\theta_E = [\pi_{rel}(4GMc^{-2}\ \mathrm{AU}^{-1})]^{1/2}$, the identification of the source reduces but does not eliminate the degeneracy in the parameters. The mass M remains entangled with π_{rel} and μ_{rel}, the lens-source relative parallax and proper motion. If the lens transits the source, one can measure μ_{rel} and so further break the degeneracy (Gould 1994). We are not able to measure μ_{rel} for PA-99-N1, but we can obtain strong constraints from the lack of finite source effects that would be induced by a transit.

Let $\rho_* = \theta_*/\theta_E$, where θ_* is the angular radius of the source. Fitting the light curve with ρ_* fixed at any value $\rho_* \leq 0.1$, we find the other parameters assume the same values as in Table 1. However, as ρ_* is increased further, t_E declines, so that the parameter combination $\rho_* t_E$ saturates at 1.0 days, and then for $\rho_* \gtrsim 0.12$, χ^2 rises dramatically. From this we derive the constraint $\rho_* t_E \leq 1.0$ days, implying $\mu_{rel} = \theta_E/t_E = \theta_*/(\rho_* t_E) \geq (\theta_*/1.0$ days). Using the empirical surface brightness/color relation of van Belle (1999), the color-color transformation of Bessell & Brett (1988), and an estimated total extinction $A_V = 0.4 \pm 0.2$, we find $\theta_* = 0.30 \pm 0.04$ μas, where the uncertainty is dominated by the 11% intrinsic scatter about the van Belle (1999) relation. The above constraint yields

$$\mu_{rel} = \frac{v_{rel}}{D_l} > 0.5\ \mathrm{km\ s^{-1}\ kpc^{-1}} \left(\frac{\rho_* t_E}{1.0\ \mathrm{days}}\right)^{-1} \left(\frac{\theta_*}{0.3\ \mu\mathrm{as}}\right), \quad (2)$$

where v_{rel} is the transverse speed of the lens relative to the observer-source line of sight and D_l is the distance to the lens. While the constraint (2) is unimportant for Galactic lenses (where $D_l \sim 10$–30 kpc), it strongly limits the allowed range of μ_{rel} for M31 lenses (since high values are exponentially suppressed). Hence, μ_{rel} is crudely measured, which implies a constrained relation between M and π_{rel}. Note that our finite source fits incorporate a linear limb-darkening parameter of 0.78 in the R band, which is appropriate for a $V-I = 2.1$ (M0–M1, 3630 K) star (Manduca, Bell, & Gustafsson 1977; Johnson 1966).

5. DISCUSSION

The location of PA-99-N1, at nearly 8′ from the center of M31, is interesting because the majority of stellar lenses are expected to reside within 5′ of the M31 center (e.g., Kerins et al. 2001). The significance of the candidate is assessed by performing Monte Carlo simulations of events with the same source magnitude, Einstein timescale, and projected position as PA-99-N1, as well as taking account of the lower limit on μ_{rel} in equation (2). We use the actual sampling and exposure times for the 1999 season. We model the halos of both galaxies with cored near-isothermal spheres, taking the mass of M31 as twice the mass of the Galaxy and assuming a core radius of 5 kpc for both galaxies. The M31 bulge follows the axisymmetric model of Kent (1989), while the disk has a sech-squared profile (see Kerins et al. 2001 for details). We base the disk stellar lens masses on the Galactic disk mass function of Gould, Bahcall, & Flynn (1997), corrected for binaries and extended down to 0.01 $M_\odot$, and the bulge stellar masses using the Zoccali et al. (2000) Galactic bulge mass function, similarly corrected and extended.

Figure 3*a* summarizes the MACHO interpretation of the event. Clearly, if the halos are full of MACHOs, the most probable interpretation is that the lens is a MACHO with mass ~0.03 $M_\odot$. This is about 5 times more likely than PA-99-N1 being due to a stellar lens. The lens is equally likely to lie in the Milky Way or M31 halo, which is quite unexpected given that the line of sight passes only 2 kpc from the center of M31 but 8 kpc from the Galactic center. Normally this would cause the M31 probability to be much higher (as shown by the thin dashed line). However, the μ_{rel} constraint (2) severely suppresses the M31 distribution at low masses while leaving the Milky Way distribution virtually unaffected. This is because the average Milky Way MACHO has a relative proper motion of ~10 km s^{-1} kpc^{-1}, while for the typical M31 MACHO it is ~0.3 km s^{-1} kpc^{-1}. The constraint also has the effect of displacing the peak of the M31 distribution toward higher mass. Assuming a logarithmic prior in the MACHO mass gives

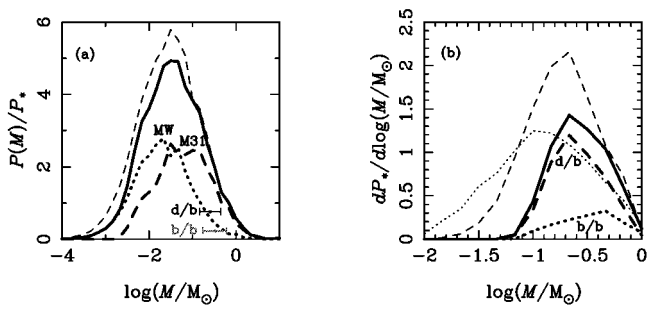

FIG. 3.—Panel (*a*) shows, for the case where PA-99-N1 is a MACHO, the probability P that the lens has mass M (*thick solid line*), normalized to the probability P_* that PA-99-N1 is a stellar lens. The contribution to this curve from M31 (Milky Way) MACHOs is shown by the thick dashed (dotted) line for full halos. The thin dashed line shows $P(M)$ for M31 MACHOs before the relative proper-motion cut (eq. [2]). The horizontal bars show the contribution to P_* from bulge-bulge lensing ("b/b") and disk-bulge lensing ("d/b"), while their width indicates the logarithmic dispersion in the stellar lens mass. Panel (*b*) shows, for the case where PA-99-N1 is a stellar lens, the overall stellar probability density as a function of lens mass (*solid line*), including the contributions from bulge-bulge lensing (*thick dotted line*) and from disk-bulge lensing (*thick dashed line*). The thin dotted and dashed lines show the relative distributions of bulge and disk lenses before the proper-motion cut.

$M = 6.4^{+21}_{-4.9} \times 10^{-2}\ M_\odot$ for an M31 MACHO and $2.1^{+7.0}_{-1.6} \times 10^{-2}\ M_\odot$ for a Milky Way MACHO (where the subscripts and superscripts refer to the 1 σ upper and lower bounds). The M31 and Milky Way distributions are both quite broad. As they are about equal in amplitude and displaced from one another by nearly a decade in mass, their combined distribution is even broader, with an FWHM extending from the planetary to the stellar mass range.

If the lens is a star, then Figure 3*b* summarizes possible interpretations. Note that the contribution of lensing involving disk sources is negligible. Allowing for the proper-motion cut, the most probable mass is around 0.2 $M_\odot$, making a rather plausible hypothesis that the lens is a low-mass star. Logarithmic averaging of the solid line gives $M = 0.27^{+0.21}_{-0.12}\ M_\odot$, i.e., only a factor of 1.8 (1 σ) uncertainty. If the lens is an M31 star, it most likely lies in the disk. This is a direct consequence of the fact that the source lies at the edge of the bulge, while the line of sight passes through the near side of the disk. Comparing Figures 3*a* and 3*b*, it is clear that the mass of the lens is much better constrained if it lies in the M31 disk than the M31 halo. This is because for M31 lenses, $M \propto (\mu_{\rm rel} t_{\rm E} D_{\rm ls})^2$, where $D_{\rm ls}$ is the distance from the lens to the source. For both populations, the product $\mu_{\rm rel} t_{\rm E}$ is reasonably well constrained, but for halo lenses, $D_{\rm ls}$ can take on a very broad range of values, while for disk lenses, the geometry implies $D_{\rm ls} = 4.0 \pm 1.8$ kpc. Since $t_{\rm E}$ is measured and $\mu_{\rm rel}$ is constrained by equation (2), M is also constrained. This means that we detect events at the location and timescale of PA-99-N1 only if the stellar mass $M > 0.1\ M_\odot(4\ {\rm kpc}/D_{\rm ls})$.

The relative rate of MACHOs to stars is subject to a number of modeling uncertainties, such as the relative mass of the Milky Way and M31 halos (Evans et al. 2000), the size of the halo core, and possibly barring of the M31 bulge. With regard to the latter, the twisting of the optical isophotes (e.g., Walterbos & Kennicutt 1987) is evidence for its presence. We note that the twisting is away from the location of PA-99-N1. We therefore expect a bar model with the same overall mass as our axisymmetric model to have a lower surface density at the position of the event and thus a lower stellar lensing rate.

6. CONCLUSIONS

We have reported the discovery of a high S/N, short-duration event that is consistent with the microlensing hypothesis. Almost certainly, the source star has been identified on archival *HST* frames, from which the Einstein crossing time of 10.4 days has been determined. We have argued—from the stability of the light curve, the achromaticity of the flux excess, the excellence of the fit, and the consistency of the color of the event at maximum with the color of the *HST* source—that by far the most natural explanation of this event is microlensing. The lens is most likely to be a MACHO if the halo fraction is above 20%. However, it is also plausible that the lens is a disk star with a mass of $\sim 0.2\ M_\odot$.

Y. L. D., E. K., E. L., and S. J. S. are supported by PPARC postdoctoral fellowships and E. L. by a CNPq postdoctoral fellowship. Work by A. G. was supported in part by a grant from Le Ministère de l'Education Nationale de la Recherche et de la Technologie and in part by grant AST 97-27520 from the NSF. We thank Sebastiano Calchi-Novati for help with the MDM data.

REFERENCES

Ansari, R., et al. 1997, A&A, 324, 843
———. 1999, A&A, 344, L49
Baillon, P., Bouquet, A., Giraud-Héraud, Y., & Kaplan, J. 1993, A&A, 277, 1
Bessell, M. S., & Brett, J. M. 1988, PASP, 100, 1134
Capaccioli, M., Della Valle, M., D'Onofrio, M., & Rosin, L. 1989, AJ, 97, 1622
Cox, A. N., ed. 2000, Allen's Astrophysical Quantities (4th ed.; New York: Springer)
Crotts, A. P. S. 1992, ApJ, 399, L43
Crotts, A. P. S., & Tomaney, A. B. 1996, ApJ, 473, L87
Demarque, P., Chaboyer, B., Guenther, D., Pinsonneault, M., Pinsonneault, L., & Yi, S. 1996, Yale Isochrones
Evans, N. W., Wilkinson, M. I., Guhathakurta, P., Grebel, E. K., & Vogt, S. S. 2000, ApJ, 540, L9
Gould, A. 1994, ApJ, 421, L71
———. 1996, ApJ, 470, 201
Gould, A., Bahcall, J. N., & Flynn, C. 1997, ApJ, 482, 913
Haiman, Z., et al. 1994, A&A, 286, 725
Johnson, H. L. 1966, ARA&A, 4, 193
Kent, S. M. 1989, AJ, 97, 1614
Kerins, E. J., et al. 2001, MNRAS, 323, 13
Le Du, Y. 2000, Ph.D thesis, Univ. Paris VI, Collège de France
Magnier, E. A., Lewin, W. H. G., van Paradijs, J., Hasinger, G., Pietsch, W., & Trümper, J. 1993, A&A, 272, 695
Manduca, A., Bell, R. A., & Gustafsson, B. 1977, A&A, 61, 809
Stetson, P. B. 1987, PASP, 99, 191
van Belle, G. 1999, PASP, 111, 1515
Walterbos, R. A. M., & Kennicutt, R. C., Jr. 1987, A&AS, 69, 311
Zheng, Z., Flynn, C., Gould, A., Bahcall, J. N., & Salim, S. 2001, ApJ, in press
Zoccali, M., Cassisi, S., Frogel, J. A., Gould, A., Ortolani, S., Renzini, A., Rich, R. M., & Stephens, A. W. 2000, ApJ, 530, 418